Proceedings of Emerging Sensing Technologies Summit 2018

Design of Deployable Helical Antennas for Space-Based Automatic Identification System Reception

Geoffrey Knott[1], Andrew Viquerat[1,*] and Alexe Bojovschi[2]

1 Department of Mechanical Engineering Sciences, University of Surrey, Guildford, GU2 7XH, United Kingdom; geoffrey.knott@surrey.ac.uk (G.K.)
2 International Innovation Research Network, Melbourne, Australia; alexe.bojovschi@iirnet.org
* Correspondence: a.viquerat@surrey.ac.uk; Tel.: +44-(0)1483-686-267

Abstract: Communications present a major bottleneck for small-satellite functionality given their extremely small volumes and low power. This work addresses this gap by presenting an ultra-compact, high-gain deployable helical antenna designed for space-based reception of Automatic Identification System signals at 162 MHz for maritime surveillance. The radio frequency characteristics of helically curved ribbons are investigated and optimized through a parametric study of the helical and ground plane geometry. Square, planar ground planes of various size and thickness, and a range of helical ribbon widths are studied. Both are modeled as perfect electrical conductors using ANSYS High Frequency Structure Simulator. Simulation results indicate that the addition of a ground plane centered and positioned at the base of the helical antenna element: 1) reduces back lobe radiation and 2) enables optimization of the radiative performance through adjusting the antenna geometry i.e. the peak gain may be increased by 3.5% (on average) for each additional helical turn — 1-8 helical turns are simulated. The half-power beam width may also be improved indefinitely by adding more helical turns. The most focused beam presented, 40 deg, is produced by an 8-turn helix, which is 58 cm in diameter and has an axial length of 3.68 m. Two ground plane sizes are considered, with the largest, which is four times larger in area, producing 5% higher peak gain. Conversely, the ground plane size had negligible effect on the half-power beam width in long helices (i.e. >3 helical turns). Increasing the helical ribbon width in steps of 10 mm was found to improve the peak gain by 8% on average in long helices.

Keywords: automatic identification system, helical, antenna, satellite, communication

---

1. Introduction

In recent years extremely small satellites have been developed in response to trends in the space industry to achieve more for less cost. By the turn of the millennium, the 'CubeSat' marked the culmination of this development enabling low-cost opportunities and ushering a new era in space experimentation [1]. A CubeSat is a cube-shaped satellite of sides 10 cm and less than 1 kg in mass, contrasting markedly to conventional satellites that are on the order of several meters and hundreds, if not thousands, of kilograms. Miniaturization, increased capability and very low power consumption electronics proved revolutionary to the semiconductor, computer and consumer electronics industries and it is intended to be as disruptive to the space industry.

Space presents multiple valuable benefits for Earth observation including forecasting the weather, assessing environmental hazards and most importantly, global coverage. However, communications remain a major bottleneck for CubeSat functionality [2]. CubeSats require compact deployable solutions given their extremely small volume and low power that restricts the size and types of antenna available for use. Typically, monopole and dipole antennas are used for telemetry and data transmission. These omnidirectional antennas operate around 146 MHz for uplink, and 437 MHz for downlink and produce low-gain characteristics (maxima of 2.06 dB and 3.35 dB, respectively [3]) providing poor data rates on the order of Kbps. Data rates a thousand times greater on the order of Mbps are required for multimedia download. High-gain antennas enable sensitive and low power communication systems. Low power consumption is crucial given the few Watts of available power in a CubeSat. Good sensitivity is important for applications where the incoming signals are weak e.g. Automatic Identification System (AIS) signals.

Utilizing the latest advances in composite materials and multi-functional deployable structures research [4], this paper presents a novel deployable helical antenna concept for enhanced space-based Automatic Identification System (S-AIS) receivers. The proposed small-satellite subsystem in Figure 1 comprises of a 10 cm x 10 cm x 10 cm cube housing five co-coiled bistable composite slit tubes (BCSTs). BCSTs are stiff and lightweight open-section tubular structures that can be rolled-up and deployed, analogous to a tape measure but without the need of any constraint to remain stowed [5]. Embedded within each of the straight and helical BCSTs are monopole and helical antennas, respectively. In addition to providing deployability and omnidirectional communications, the straight BCSTs support a gossamer ground plane for improved radio frequency (RF) characteristics i.e. gain and directionality, and to minimize backlobes of the helical antenna.

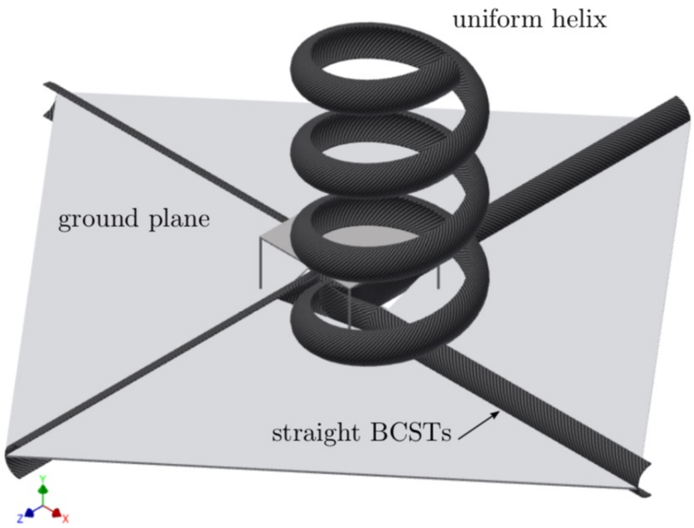

Figure 1. Conceptualized small-satellite S-AIS receiver comprising of straight and helical embedded deployable antennas, and gossamer ground plane.

The paper is organized as follows: Section 2 outlines the helical antenna design theory and simulation approach used, and an example of RF results and their interpretation; Section 3 presents RF simulation results (i.e. the peak gain, half-power beam width and reflection coefficient versus number of helical turns, ground plane size and thickness and helical ribbon width); Section 4 evaluates the effectiveness of each antenna parameter for optimizing the RF characteristics.

2. Method

The helical antenna investigated in this work is designed for receiving S-AIS signals in axial mode at 162 MHz and based on Kraus' formulas [6]. These formulas estimate the antenna peak gain and directionality, presented in (1)-(5), and highlight the large size antenna required for operation at such low frequencies e.g. AISat [7,8]. In the literature these formulas have been shown as too optimistic [9] whilst those from Emerson in (A1) [10] are too pessimistic and those empirically derived by Wong & King in (A2) & (A3) [11] lying in-between Kraus' and Emerson's estimations. As a result of the range in predicted effects of helical geometry on RF characteristics, these additional formulas are plotted in the RF results for comparison — the formulas are shown in Appendix A. The Kraus design equations for an axial mode helical antenna [6] are,

$$C = \lambda = 1.85\,\text{m} \tag{1}$$

$$S = \frac{\lambda}{4} = 0.46\,\text{m} \tag{2}$$

$$R = \frac{\lambda}{2\pi} = 0.29\,\text{m} \tag{3}$$

where C is the helical circumference, S is the spacing between each turn of helix, and R is the helical radius. A 7-turn helical antenna is modeled ($N = 7$) that is predicted to produce a peak gain (G, a measure of efficiency) and half-power beam width ($HPBW$, a measure of directionality) of:

$$G = 10.8 + 10\log\left(\frac{NC^2S}{\lambda^3}\right) = 13.2\,\text{dBi} \tag{4}$$

$$HPBW = \frac{52^\circ}{C}\sqrt{\frac{\lambda^3}{NS}} = 39.4^\circ \tag{5}$$

In order to evaluate the potential 162 MHz S-AIS reception performance of the helical antenna, ANSYS High Frequency Structure Simulator (HFSS) [12] is used to model, simulate, and determine RF properties including radiation pattern (i.e. peak gain and HPBW) and bandwidth. The antenna material is modeled as a helically curved ribbon of perfect electrical conductor — the ground plane is also modeled as perfect conductor material. A suitable feed line is modeled and excited using a lumped port with matched impedance of 50 Ω. Due to ground plane effects on the achievable antenna gain and directionality, two sizes of square, planar ground plane are simulated with sides of 1.39 m ($3\lambda/4$ m) and 2.78 m (1.5λ m). One case for the total gain and radiation pattern is presented in Figure 2 for a 7-turn helix of width 20 mm, with a 1.5λ m-sided ground plane, which is 10 mm thick. This simulation result indicates a peak gain of 11.35 dBi and HPBW of 46 deg, which differ from the optimistic theoretical values calculated in (1)-(5) due to neglecting additional RF effects caused by the ground plane and helical ribbon geometries. The reflection coefficient for the 7-turn helix with a 2.78 m-sided ground plane is presented in Figure 3, indicating operation at AIS frequency (i.e. S11 < -10 dB at 162 MHz). However, future antenna designs would need further optimization in order to decrease the bandwidth, which currently spans a large range due to S11 < -10 dB from 70 MHz to 1 GHz. However, optimizing the peak gain and HPBW are primary focus in this work and this simulation setup is used to produce the RF results for N-turn helical antennas.

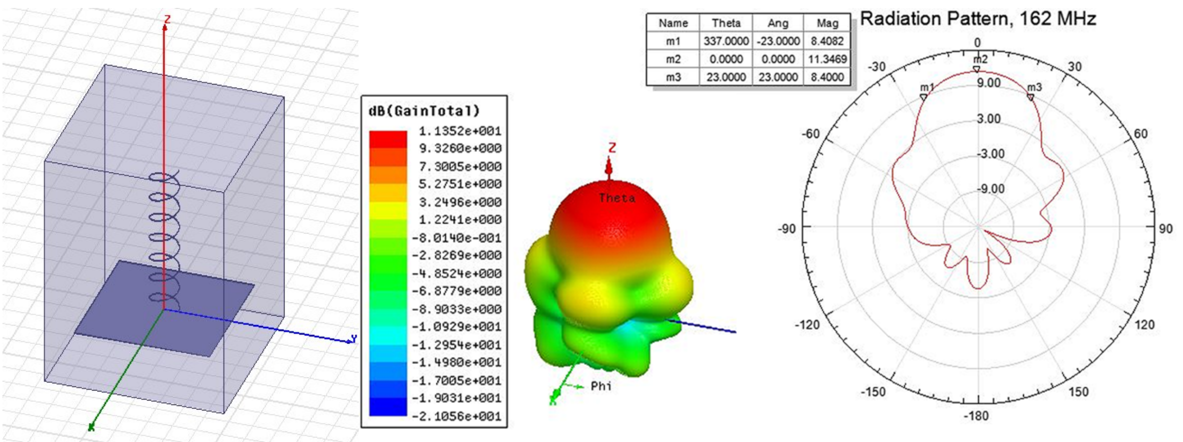

Figure 2. HFSS simulation setup and RF results for a 7-turn helical antenna as outlined

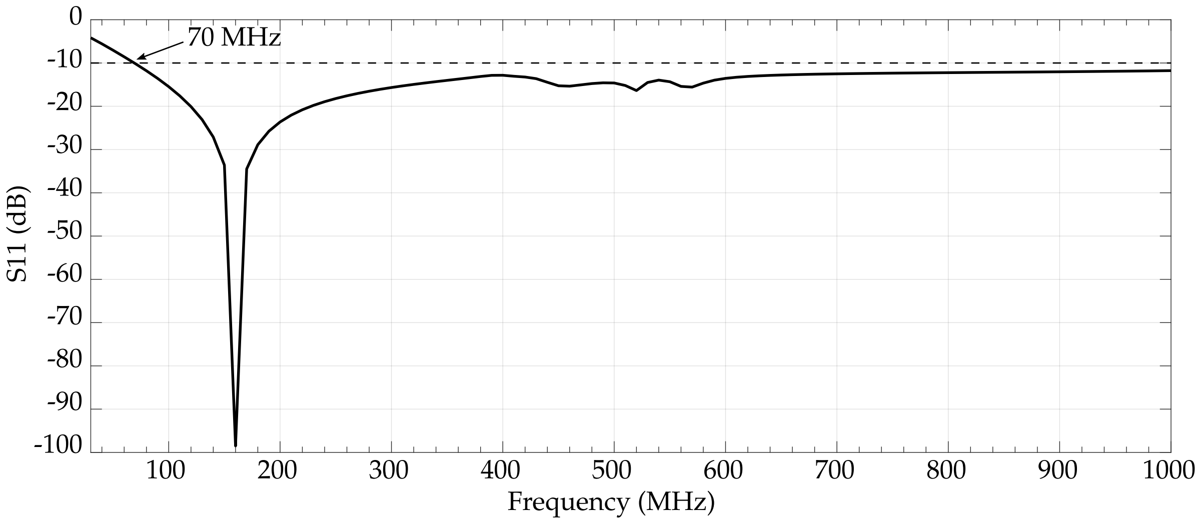

Figure 3. Reflection coefficient, S11, versus frequency for a 7-turn helix. A square ground plane of sides 2.78 m and helical ribbon width of 20 mm is modeled

3. Results

The RF result for a helical antenna without ground plane is presented in Figure 4. RF simulation results for four helical antennas with square, planar ground planes with sides $3\lambda/4$ and 1.5λ m, and thickness 10 and 2 mm are presented in Figure 5 — predictions from the literature [6,10,11] are included. The helical antenna is modeled as a helically curved ribbon with the RF simulation results for various ribbon widths (i.e. 10, 20, 30, 40, and 50 mm) presented in Figure 6. The antenna reflection coefficients versus frequency for each ribbon width are presented in Figure 7.

4. Discussion

The radiation pattern produced by a helical antenna without ground plane achieves low gain and poor directionality (i.e. large HPBW) as shown in Figure 4. The standalone 7-turn helix produces two radiation lobes oriented along the helical axis, along the 'Z' axis where 'Theta' equals zero and 180 degrees. The largest of these lobes is back-facing and exhibits a peak gain of 3.7 dBi, and a very large HPBW of 172 deg. Such a HPBW would be too high for effective targeted sensing applications such as S-AIS signals reception. The radiation pattern and peak gain are relatively constant and independent from the number of helical turns.

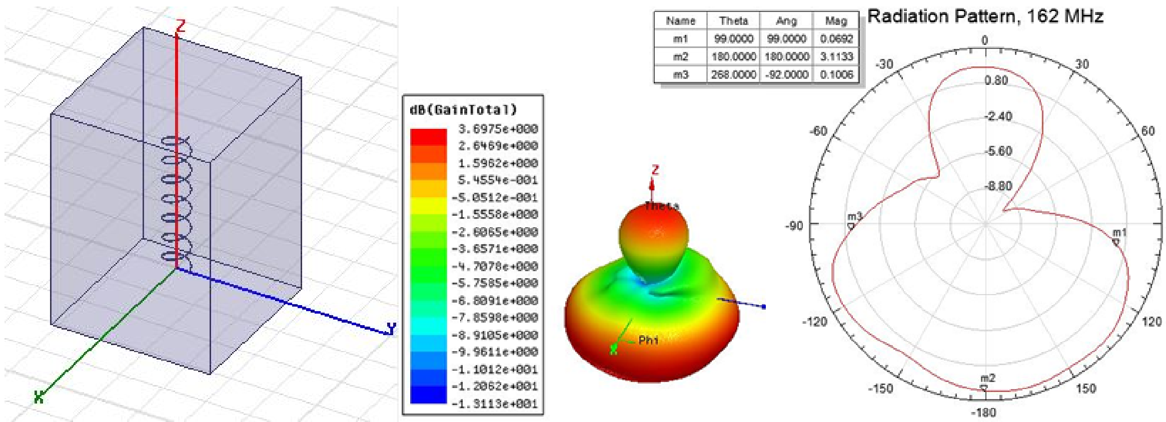

Figure 4. HFSS simulation setup and RF radiation pattern of a helical antenna without ground plane

Introducing a ground plane reduces and reflects the back lobe radiation along the 'Z' or 'Theta'= 0 axis and enables the optimization of the gain and HPBW through the addition of more helical turns. This is the most effective approach for RF improvement in deployable structures such as BCSTs, and achievable relatively straightforwardly by extending the total length of the antenna whilst minimally increasing in the packaged size.

Helical antennas with two sizes of square, planar ground plane were simulated with sides of $3\lambda/4$ and 1.5λ m to investigate effects on the RF properties, as shown in Figure 5 (solid and dashed, black and red lines). In contrast to the standalone helix, a single main lobe is oriented along the axis of the helix. In addition to producing a forward-facing main lobe, the gain and directionality may be affected by the number of helical turns to present design flexibility. The parametric study shows that for each additional helical turn an average increase of 3.5% in the peak gain is observed. (This occurs for both sizes of ground plane.) Comparing the two sizes of more directly, the gain produced by the larger ground plane (1.5λ m) is 5% higher on average over the range of helical turns simulated. This is likely a result of the 1.5λ m ground plane reflective surface area that is four times greater than the $3\lambda/4$ m, however, a modest 5% increase may indicate that enlarging the ground plane may not be the mass-optimal method for RF improvement in small satellites.

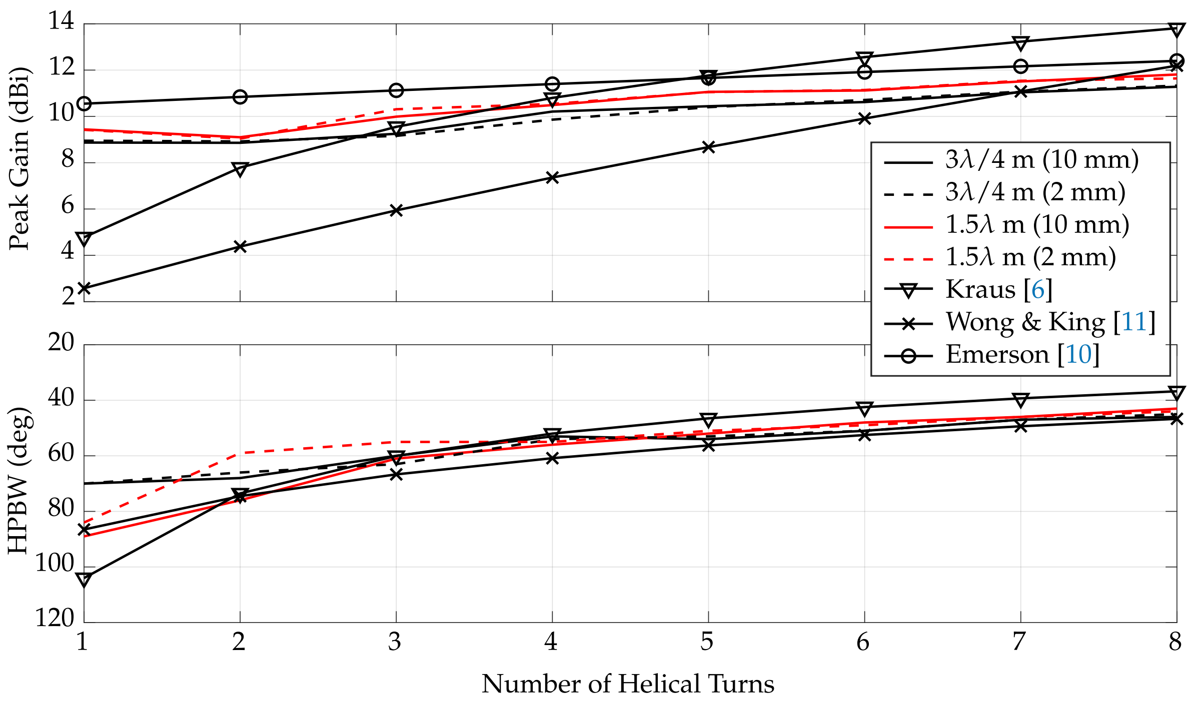

Figure 5. Effect of ground plane size ($3\lambda/4$ and 1.5λ m) and thickness (10 and 2 mm) on peak gain and HPBW. Predictions from literature [6,10,11] are included. The helical ribbon width simulated is 20 mm

The HPBW produced by the larger ground plane is also superior up to $N \leq 4$ helical turns after-which it is the smaller ground plane that achieves a narrower beam (-3 deg). Initially this appears counter intuitive with a presumption that the bigger the better, however this is false.

These results highlight the complex coupling between the geometry of the helical element (i.e. number of turns and ribbon width) and the ground plane (i.e. size and thickness). Kraus in [6] outlined specific bounds in the helical design space for the helical circumference ($0.7\lambda < C < 1.3\lambda$), helical spacing ($0.01\lambda < S < 0.5\lambda$) and pitch angle ($12° < \alpha < 15°$) required to achieve at least axial-mode operation — these were used previously in (1)-(5) and are plotted in Figure 5 (black solid line with triangular markers). Kraus' predictions, which are strictly valid for $N > 3$ helical turns, overestimate the gain and HPBW for $N \geq 4$ helical turns by up to $+2.5$ dBi and -9 deg, respectively.

Although the generally pessimistic peak gain formula from Emerson [10] is strictly valid for $2 < \mathrm{L}/\lambda < 7$ and $S/\lambda = 0.24$, where L/λ is the axial length of the helix in wavelengths, the parallel trend in the range $4 \leq N \leq 8$ (i.e. the solid black line with circular markers) consistently over-predicts the gain by $+0.71$ and $+1.19$ dBi for the 1.5λ and 0.75λ m ground planes, respectively. (For clarification, the helical turns considered in this work, $1 \leq N \leq 8$, equate to $0.25 \leq L/\lambda \leq 2$.) This factor could be readily adjusted in A1 for better predictions, however, the original formula is presented in this case. The peak gain results converge to Emerson's predictions, which can be explained by the latter's assumption of an infinitely sized ground plane.

The complexity of antenna design with specific consideration of the ground plane is underlined further by Djordjevic in [13] who showed that a square ground plane of sides 1.5λ m could outperform an infinite one in terms of maximizing the average peak gain over the frequency range considered (i.e. 1.2-2.2 GHz). The empirically derived formulas from Wong & King [11] (i.e. solid black lines with 'x' markers) are based on helical antennas operating in the 650-1,100 MHz frequency range, with $5 \leq N \leq 35$ helical turns, 5 mm-diameter copper tubing and a high circular cavity rather than a conventional ground plane. Although these formulas will not be valid for the antennas designed in this work for 162 MHz and with square, planar ground planes — this is particularly apparent in comparing the peak gain values — the HPBW predicted by Wong & King closely match with a minor discrepancy of -1.46 deg.

Two ground plane thicknesses (10 and 2 mm) are also presented in Figure 5, which are simulated to investigate the effects of using extremely thin material for the envisaged reflective membrane. (The ground plane must be very thin, typically less than 1 mm, for ultra-compact folding and stowage inside a small satellite.) The results show that particularly for $N \geq 5$ helical turns (>10.5 dBi) the ground plane thickness has negligible effect on gain. Furthermore, the HPBW is relatively unaffected by the ground plane thickness for $N \geq 4$ turns. These results provide confidence in using thin materials for the ground plane that both minimize mass and maximize stowed-to-deployed volume ratio without compromising the RF characteristics.

Further RF improvements may be achieved by increasing the width of the helical ribbon as shown in Figure 6. The helical ribbon widths simulated are 10-50 mm, in steps of 10 mm. Firstly, the results confirm that increasing the number of helical turns significantly improves the peak gain and HPBW. The RF results for $N \leq 3$ and $N \geq 3$ helical turns exhibit increases in the peak gain to various degrees. It is observed that for short helices with $N \leq 3$ helical turns, expanding the ribbon width in steps of 10 mm produces a modest 2% increase in peak gain on average. Comparing the peak gain produced by long helical antennas (i.e. $3 \leq N \leq 8$ turns) with ribbon widths of 10 and 50 mm, the peak gain is improved more significantly by 8% on average, indicating that increasing the ribbon width is far more effective in long helical antennas (i.e. $N \geq 3$). The greatest peak gain increase is observed at $N = 8$ helical turns for 10 to 50 mm ribbon width, from 11.23 to 12.52 dBi, representing an increase of 11.5%. Figure 7 confirms that the antennas continue to operate at each helical ribbon width due to S11 < -10 dB at 162 MHz.

It has been established that the HPBW decreases with the number of helical turns as the main lobe is enhanced and narrowed. This is essential for directional antenna, or targeted, sensing applications. The HPBW rapidly improves for $N < 3$ turns, with much shallower and constant narrowing for $N > 3$ turns (Figure 6). The HPBW may be decreased indefinitely by increasing the number of turn and/or ribbon width. In these simulations the lowest HPBW is 40 deg for $N = 8$ helical turns and 50 mm ribbon width.

5. Conclusions

A deployable helical antenna is presented and its RF properties investigated through a parametric study of the helical and ground plane geometry. Mass-optimal approaches for optimizing the RF performance are identified. The antenna structure is envisaged to be manufactured using bistable

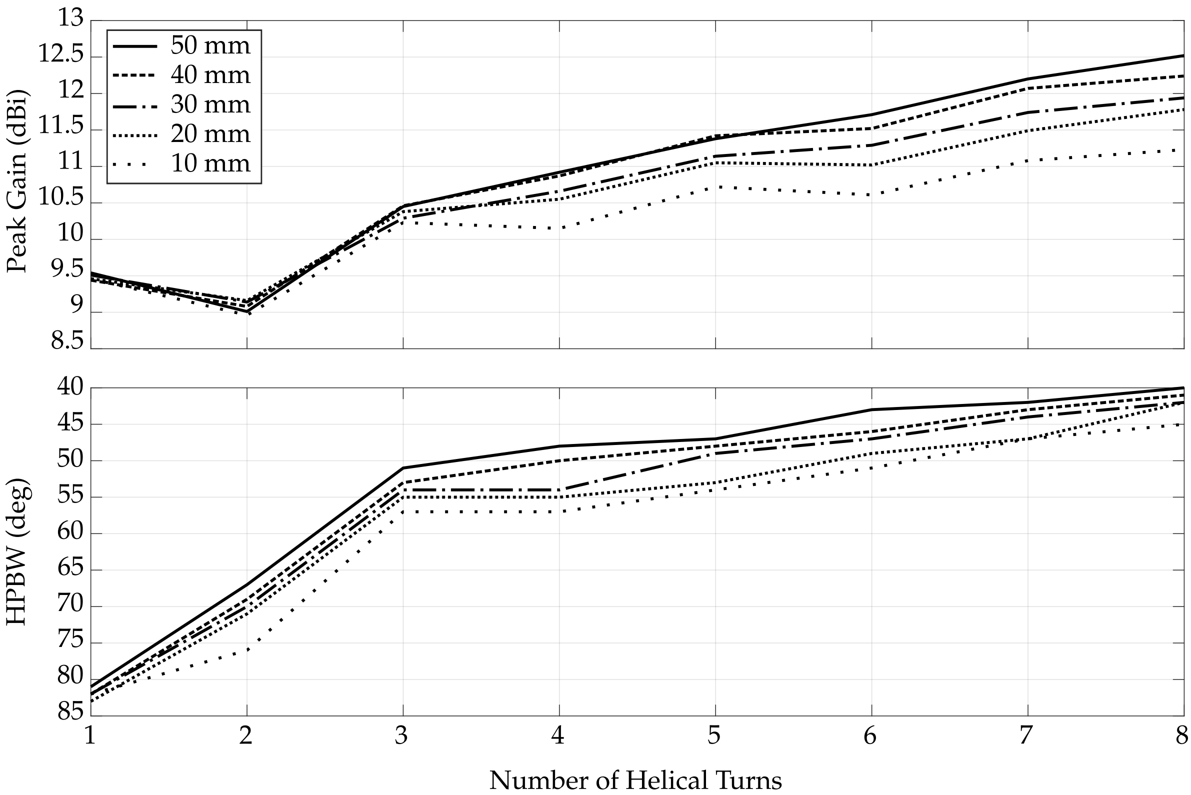

Figure 6. Effect of helical ribbon width on gain and HPBW. A ground plane thickness of 1 mm is simulated

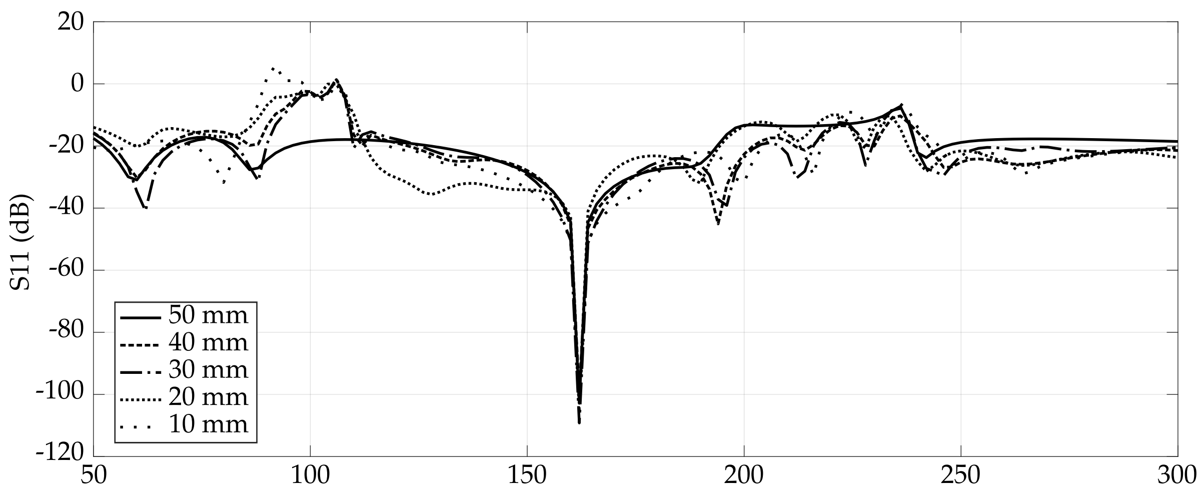

Figure 7. Effect of helical ribbon width on the reflection coefficient, S11

composite to enable extremely compact stowage. Conducting material such as copper shall be embedded to provide the radiative element.

Further work is required for RF simulations of helical tubes to investigate additional geometrically dependent RF effects. This is achievable by introducing cross-sectional curvature into the helically curved ribbons modeled thus far. Additionally, due to the deployment method of the helical antenna element, the helix may in practice be positioned off-center with respect to the center of the ground plane — this shall be considered in future for quantifying affects on the main lobe direction and magnitude. This could be addressed using appropriate feed lines. Addressing these two points may better represent the RF characteristics of the helical tube antenna architecture envisaged.

The square gossamer ground plane architecture presented here comprises of four distinct quadrants. Therefore, addition investigations are required to identify the consequences segmenting the ground plane may incur on RF performance. Furthermore, parabolic ground planes may be investigated for enhanced gain and HPBW, which can enable more compact ground planes to achieve comparable RF properties to planar, square architectures.

Finally, given that the helical copper ribbon considered thus far is an element embedded within a helical composite structure, incorporating additional structural materials into the simulated antenna such as carbon-fiber, may be considered to identify a potential source of RF interference or amplification.

Funding: This research was funded by the Engineering and Physical Sciences Council, UK Research and Innovation, grant number EP/R044902/1. Dr Geoffrey Knott thanks Dr Andrew Viquerat, the Faculty of Engineering and Physical Sciences at the University of Surrey and organizers of the Emerging Sensing Technologies Summit (ESTS 2018), particularly Dr Alexe Bojovschi, for conference funding contributions.

Abbreviations

The following abbreviations are used in this manuscript:

S-AIS	space-based Automatic Identification System
BCST	bistable composite slit tube
RF	radio frequency
AIS	Automatic Identification System
HPBW	half-power beam width
HFSS	High Frequency Structure Simulator
ESTS	Emerging Sensing Technologies Summit

Appendix A. Helical antenna design equations

The peak gain formula from Emerson [10] in units of dBi is,

$$G_{Emerson} = 10.25 + 1.22\frac{\mathrm{L}}{\lambda} - 0.0726\left(\frac{\mathrm{L}}{\lambda}\right)^2 \tag{A1}$$

where L/λ is the axial length of the helix in wavelengths, and the formulas from Wong & King [11], including HPBW in units of degrees, are,

$$G_{Wong\ \&\ King} = 8.3\left(\frac{\pi \mathrm{D}}{\lambda}\right)^{\sqrt{N+2}+1}\left(\frac{NS}{\lambda}\right)^{0.8}\left[\frac{\tan 12.5}{\tan\alpha}\right]^{\sqrt{N}/2} \tag{A2}$$

$$\mathrm{HPBW}_{Wong\ \&\ King} = \frac{61.5\left(\frac{2N}{N+5}\right)^{0.6}}{\left(\frac{\pi \mathrm{D}}{\lambda}\right)^{\sqrt{N}/4}\left(\frac{NS}{\lambda}\right)^{0.7}}\left[\frac{\tan\alpha}{\tan 12.5}\right]^{\sqrt{N}/4} \tag{A3}$$

where D is the helical diameter (i.e. $2R$), λ is the wavelength, N is the number of helical turns, S is the helical spacing, and α is the helical pitch angle (i.e. $S = \pi \mathrm{D}\tan\alpha$).

References

1. Heidt, H.; Puig-Suari, J.; Moore, A.S.; Nakasuka, S.; Twiggs, R.J. CubeSat: A new Generation of Picosatellite for Education and Industry Low-Cost Space Experimentation. 14th Annual/USU Conference on Small Satellites, 2000, pp. 1–19.

2. Muri, P.; Challa, O.; McNair, J. Enhancing Small Satellite Communication Through Effective Antenna System Design. The 2010 Military Communications Conference. IEEE, 2010, pp. 347–352. doi:10.1109/MILCOM.2010.5680405.
3. Schraml, K.; Narbudowicz, A.; Chalermwisutkul, S.; Heberling, D.; Ammann, M. Easy-to-deploy LC-loaded dipole and monopole antennas for cubesat. 11th European Conference on Antennas and Propagation (EUCAP), 2017, pp. 2303–2306. doi:10.23919/EuCAP.2017.7928135.
4. Knott, G.; Viquerat, A. Helical bistable composite slit tubes. *Composite Structures* **2019**, *207*, 711–726. doi:10.1016/j.compstruct.2018.09.045.
5. Iqbal, K.; Pellegrino, S.; Daton-Lovett, A. Bi-stable Composite Slit Tubes. In *Solid Mechanics and Its Applications*; Pellegrino, S.; Guest, S.D., Eds.; Springer, Dordrecht, 2000; chapter IUTAM-IASS Symposium on Deployable Structures: Theory and Applications, pp. 153–162. doi:10.1007/978-94-015-9514-8_17.
6. Kraus, J., Ed. *Antennas for all Applications*, 3rd ed.; McGraw-Hill, Inc., 2003.
7. Spröwitz, T.; Block, J.; Bäger, A.; Hauer, L.; Schütze, M. Deployment Verification of Large CFRP Helical High-Gain Antenna for AIS Signals. IEEE Aerospace Conference Proceedings, 2011. doi:10.1109/AERO.2011.5747319.
8. Block, J.; Bäger, A.; Behrens, J.; Delovski, T.; Hauer, L.C.; Schütze, M.; Schütze, R.; Spröwitz, T. A self-deploying and self-stabilizing helical antenna for small satellites. *Acta Astronautica* **2013**. doi:10.1016/j.actaastro.2011.10.012.
9. Djordjević, A.R.; Zajić, A.G.; Ilić, M.M.; Stüber, G.L. Optimization of Helical Antennas. *IEEE Antennas and Propagation Magazine* **2006**, *48*, 107–116. doi:10.1109/MAP.2006.323359.
10. Emerson, D.T. THE GAIN OF THE AXIAL-MODE HELIX ANTENNA: A NUMERICAL MODELING STUDY.
11. Wong, J.L.; King, H.E. Empirical Helix Antenna Design. Antennas and Propagation Society International Symposium, 1982, pp. 366–369. doi:10.1109/APS.1982.1148836.
12. ANSYS, Inc.. ANSYS Electromagnetics Suite 18.0.0, 2018.
13. Djordjević, A.R.; Zajić, A.G.; Ilić, M.M. Enhancing the Gain of Helical Antennas by Shaping the Ground Conductor. *IEEE Antennas and Wireless Propagation Letters* **2006**, *5*, 138–140. doi:10.1109/LAWP.2006.873946.